2020/06/03
Archive Hash: eb7aff9-D
Archive Date: 2020/06/02

Observation of forward neutron multiplicity dependence of dimuon acoplanarity in ultra-peripheral PbPb collisions at $\sqrt{s_{\mathrm{NN}}} = 5.02\,\mathrm{TeV}$

The CMS Collaboration

Abstract

The first measurement of forward neutron multiplicity dependence of $\gamma\gamma \to \mu^+\mu^-$ production in ultra-peripheral PbPb collisions at $\sqrt{s_{\mathrm{NN}}} = 5.02\,\mathrm{TeV}$ is reported by the CMS experiment at the LHC. The azimuthal correlations between two muons in the invariant mass region $8 < M_{\mu\mu} < 60\,\mathrm{GeV}$ are extracted for events associated with zero, one, or at least two neutrons produced in the very forward region. The strong back-to-back correlation structure from leading-order photon-photon scattering is significantly broadened for events producing a larger number of neutrons from each nucleus, corresponding to interactions having a smaller impact parameter. This observation demonstrates that the transverse momentum and energy of photons emitted from relativistic ions have impact parameter dependence. These results constrain ~~precision modeling~~ models of initial photon-induced interactions in ultra-peripheral collisions. They also provide a controllable baseline to search for possible final-state effects on lepton pairs resulting from the production of quark-gluon plasma in hadronic heavy ion collisions.

The Lorentz boosted electromagnetic (EM) fields surrounding relativistic heavy ions with large charges (Z) can be treated as a flux of linearly polarized quasi-real photons [1, 2] with flux intensity proportional to Z^2. Therefore, two ions can still interact when their impact parameter (b) is greater than twice the nuclear radius, so-called ultra-peripheral collisions (UPC). These EM interactions include photon-photon and photon-nucleus processes [3–8]. Two-photon collisions are fundamental processes, which can be used to test quantum electrodynamics (QED) and to search for physics beyond the standard model [6–11]. Photon-nucleus interactions allow a direct measurement of the gluon distribution in the nucleon or nucleus [6–8], especially for small Bjorken x at Large Hadron Collider (LHC) energies.

These two types of photon-induced interactions can occur in conjunction with the excitation of one or both of the ions via absorption of photons into giant dipole resonances (GDRs) or other higher excited states [6–8, 12, 13]. The GDRs typically decay by emitting a single neutron, while higher excited states may emit two or more neutrons. These neutrons have very low relative momentum with respect to their parent ions, and therefore approximately retain the beam rapidity. The contribution of higher excitations becomes larger as b gets smaller [6–8]. Therefore, the number of emitted neutrons in the forward region can be used to classify UPC events into different impact parameter ranges, a concept analogous to the centrality commonly determined in hadronic ~~heavy-ion~~ heavy ion interactions. Higher neutron multiplicity corresponds to smaller ~~$\langle b \rangle$ on average~~ average b, and vice versa [6–8].

The momentum of emitted quasi-real photons is predominantly along the beam direction and has transverse momentum (p_{T}) on the scale of ω/γ_L, where ω is the photon energy and γ_L is the Lorentz factor of the projectile and target nuclei. The lepton pairs produced from leading-order photon-photon scattering ($\gamma\gamma \to \ell^+\ell^-$) possess small pair p_{T} and are nearly back-to-back in azimuth ~~angles~~ angle (ϕ). Photon-induced interactions have been extensively studied in UPC collisions [14–23]. Recently, photon-photon [24, 25] and photon-nucleus [26, 27] processes have also been observed at very low p_{T} in hadronic ~~heavy-ion~~ heavy ion collisions at the Relativistic Heavy Ion Collider (RHIC) and the LHC. Products from photon-induced interactions have been proposed as a tool to study the properties of a deconfined state of partonic matter, known as quark-gluon plasma (QGP). In particular, the p_{T} [24] and azimuthal angular correlations [25] of lepton pairs produced via photon-photon scattering in hadronic events show a broadening effect compared to that from vacuum production in UPC events. Final-state EM modifications (e.g., Coulomb rescattering, or deflection by magnetic fields trapped in a QGP) of lepton pairs in the presence of a QGP medium have been proposed as possible interpretations of the broadening effect [24, 25, 28]. However, a QED calculation indicates that the observed broadening effect can be largely explained by p_{T} hardening of initial-state photons as the impact parameter decreases toward central hadronic collisions [29]. Another QED calculation, predicting different b dependence of the initial photon p_{T}, is discussed in Ref. [30]. To disentangle possible contributions from initial- and final-state effects to the modifications observed in hadronic ~~heavy-ion~~ heavy ion collisions, an experimental handle on the impact parameter dependence of lepton pair production in UPC collisions is essential. Establishing possible impact parameter dependence of initial photon energy and p_{T} would also pave the way for future high precision modeling of photon-induced interactions for studies of initial nuclear effects [6–8] and searches for physics beyond the standard model [7, 9–11].

This letter reports the first measurement of the forward neutron multiplicity dependence of $\gamma\gamma \to \mu^+\mu^-$ production in the muon pair invariant mass region $8 < M_{\mu\mu} < 60\,\mathrm{GeV}$ in ultra-peripheral lead-lead (PbPb) collisions at a nucleon-nucleon center-of-mass energy ($\sqrt{s_{\mathrm{NN}}}$) of 5.02 TeV, using data collected with the CMS detector during the 2018 LHC run. The PbPb sample corresponds to an integrated luminosity of approximately 1.5 nb^{-1}. Azimuthal correlations

of muon pairs, or acoplanarity (α) defined as

$$\alpha = 1 - \frac{|\phi^+ - \phi^-|}{\pi}, \tag{1}$$

are presented for several different classes of neutron multiplicity detected in the very forward region. Here, $\phi^{\pm}$ represent the azimuthal angles of two muons. The α of the lepton pair produced from leading-order $\gamma\gamma$ scattering is directly related to the lepton pair p_{T}, which is equal to the total p_{T} of the initial photons. Thus, the large $\langle\alpha\rangle$ of lepton pairs produced from leading-order $\gamma\gamma$ scatterings corresponds to large $\langle p_{\mathrm{T}}\rangle$ of the initial photons, and vice versa. The average invariant mass of all muon pairs from $\gamma\gamma$ interactions in various neutron multiplicity classes is also measured.

The central feature of the CMS apparatus is a superconducting solenoid of 6 m internal diameter, providing a magnetic field of 3.8 T. Within the solenoid volume, there are four primary subdetectors including a silicon pixel and strip tracker detector, a lead tungstate crystal electromagnetic calorimeter, and a brass and scintillator hadron calorimeter, each composed of a barrel and two endcap sections. Muons are detected in the pseudorapidity interval of $|\eta| < 2.4$ in gas-ionization detectors embedded in the steel flux-return yoke outside the solenoid, with detection planes made using three technologies: drift tubes, cathode strip chambers, and resistive plate chambers. Matching muons to tracks measured in the silicon tracker leads to a relative p_{T} resolution around 1% [31] and an azimuthal angle resolution better than 7×10^{-4} radians for a typical muon in this analysis. CMS has extensive forward calorimetry, including two steel and quartz-fiber Cherenkov hadron forward (HF) calorimeters that cover the range of $2.9 < |\eta| < 5.2$, which are used to reject hadronic PbPb collision events. Two zero degree calorimeters (ZDC), made of quartz fibers and plates embedded in tungsten absorbers, are used to detect neutrons from nuclear dissociation events in the range $|\eta| > 8.3$. A detailed description of the CMS detector, together with a definition of the coordinate system used and the relevant kinematic variables, can be found in Ref. [32].

Events used in this measurement were selected by a fast hardware-based trigger system that requires at least one muon candidate coincident with a PbPb bunch crossing. There is no explicit selection on the muon p_{T}. Events with an energy deposit above noise threshold in both HF calorimeters are vetoed. For the offline analysis, events have to pass a set of selection criteria designed to reject beam-related background processes (beam-gas collisions and beam scraping events) and hadronic collisions. Events are required to have a valid primary interaction vertex and the shapes of the clusters in the pixel detector have to be compatible with those expected from particles produced by a PbPb collision [33]. To suppress hadronic PbPb collisions, the largest energy deposits in the HF calorimeters are required to be below 7.3 GeV and 7.6 GeV in the positive and negative rapidity sides, respectively, where these noise thresholds are determined from empty bunch crossing events. In addition, events must contain exactly two muon candidates and no additional track in the range $|\eta| < 2.5$. Selected events are then classified by neutron multiplicity, which is determined by the energy deposited in the ZDCs. The total energy distribution is divided into three neutron multiplicity classes (0n, 1n, and Xn with $X \geq 2$) on each side with energy thresholds. The corresponding purities are estimated by a multi-Gaussian function fit to the energy distribution. The purities are nearly 100% for the 0n and Xn classes and ~93–95% for the 1n class. From the combinations of the number of neutrons in each ZDC separately, a total of six neutron multiplicity classes, labeled as 0n0n, 0n1n, 0nXn, 1n1n, 1nXn, and XnXn, are used in this measurement. The 0n0n class corresponds to no Coulomb break-up of either nucleus and the 1nXn class corresponds to one neutron emitted from one nucleus and at least two neutrons emitted from the other nucleus.

Muons are selected in the kinematic range of $p_{\mathrm{T}}^{\mu} > 3.5\,\mathrm{GeV}$ and $|\eta^{\mu}| < 2.4$. They are reconstructed using the combined information of the tracker and muon detectors (so-called "soft muons" defined in Ref. [31]). The opposite sign (OS) distribution (signal and background) is reconstructed by combining μ^+ and μ^- candidates, while the background is estimated by combining the same charge sign (SS) muons in the same event. Each OS or SS pair must contain at least one muon candidate matched to a triggered muon. The studied dimuon kinematic range is limited to $8 < M_{\mu\mu} < 60\,\mathrm{GeV}$ and rapidity $|y^{\mu\mu}| < 2.4$. This mass region is selected to suppress the contribution from photoproduced resonances (charmonia and Z ~~boson~~bosons) decaying to $\mu^+\mu^-$ pairs, and to avoid large efficiency corrections.

The detector performance is estimated by a dedicated $\gamma\gamma \to \mu^+\mu^-$ Monte Carlo (MC) simulation sample produced with the STARlight (v3.0) event generator [34] without restriction on Coulomb break up for each nucleus. In STARlight, only $\ell^+\ell^-$ pairs from the leading-order $\gamma\gamma$ scattering are generated, and the calculation is performed by integrating over the entire impact parameter space for UPC events. No differential impact parameter dependence of initial photon p_{T} is considered in STARlight. The CMS detector response is simulated using GEANT4 [35]. To account for the strong kinematic correlation between μ^+ and μ^- produced from $\gamma\gamma$ scattering, the muon reconstruction and trigger efficiencies are applied as ~~a function~~ functions of p_{T}^{μ}, η^{μ}, and ϕ^{μ}. To correct for detector inefficiencies, each muon pair is weighted by $(\varepsilon_{trig} \times \varepsilon_{reco})^{-1}$, where $\varepsilon_{trig} = 1 - (1 - \varepsilon_{trig}^{\mu^+})(1 - \varepsilon_{trig}^{\mu^-})$ and $\varepsilon_{reco} = \varepsilon_{reco}^{\mu^+} \times \varepsilon_{reco}^{\mu^-}$. The reconstruction and trigger efficiencies rapidly reach a plateau as functions of p_{T} with values of ~95–99% at $p_{\mathrm{T}}^{\mu} \approx 6\,\mathrm{GeV}$ for $|\eta^{\mu}| < 1.2$ and $p_{\mathrm{T}}^{\mu} \approx 4\,\mathrm{GeV}$ for $1.2 < |\eta^{\mu}| < 2.4$. Systematic uncertainties associated with efficiency corrections are negligible since they largely cancel out in final observables, which are normalized by the total yield.

The cross section of single electromagnetic dissociation (EMD) [36, 37] of Pb nuclei in PbPb collisions is measured to be 187.4 ± 0.2 (stat.) $^{+13.2}_{-11.2}$ (syst.) b at $\sqrt{s_{\mathrm{NN}}} = 2.76\,\mathrm{TeV}$ [38] and is expected to be even larger at $\sqrt{s_{\mathrm{NN}}} = 5.02\,\mathrm{TeV}$ due to stronger EM fields. Because of the large single EMD cross section, a single measured $\gamma\gamma \to \mu^+\mu^-$ event may contain concurrent EMD events. These concurrent events can emit neutrons and migrate the neutron multiplicity of a single $\gamma\gamma \to \mu^+\mu^-$ interaction to higher values. This EMD pileup effect is quantified by measuring ZDC energy distributions from "zero bias" triggered events that only require the presence of both beams in the same bunch crossing. No valid collision vertex and track is allowed to be present in the event. However, the same HF veto thresholds as the $\gamma\gamma \to \mu^+\mu^-$ events are applied. The neutron multiplicity classes in these zero bias events are used to estimate the probabilities of a $\gamma\gamma \to \mu^+\mu^-$ event being classified into an incorrect neutron multiplicity class because of pileup effects. By inverting a matrix of these migration probabilities, the true observable distributions are extracted from the measured data. About 11.0% of measured $\gamma\gamma \to \mu^+\mu^-$ events have neutron multiplicity migration caused by EMD pileup.

Figure 1 shows the corrected α distributions of $\mu^+\mu^-$ pairs in PbPb collisions for different neutron multiplicity classes within the CMS acceptance ($p_{\mathrm{T}}^{\mu} > 3.5\,\mathrm{GeV}$, $|\eta^{\mu}| < 2.4$, and $|y^{\mu\mu}| < 2.4$). The α distributions are normalized to unit integral over their measured range ($(1/N_s)dN_s/d\alpha$, N_s represents signal yield). Each α spectrum is made up of a narrow core close to zero and a long tail, where the core component mostly originates from the leading-order $\gamma\gamma$ scattering while in the tail component ~~mostly originates from~~ , high-order $\gamma\gamma$ processes predominate. These high-order processes include, for example soft photon radiations off the produced lepton and scattering of multiple photons [5, 28]. The tail contribution in the $X\mathrm{n}X\mathrm{n}$ class is larger than that in the 0n0n class. This is consistent with the expectation of larger contributions of high-order $\gamma\gamma$ processes in UPC events that have smaller impact ~~parameter~~ parameters and

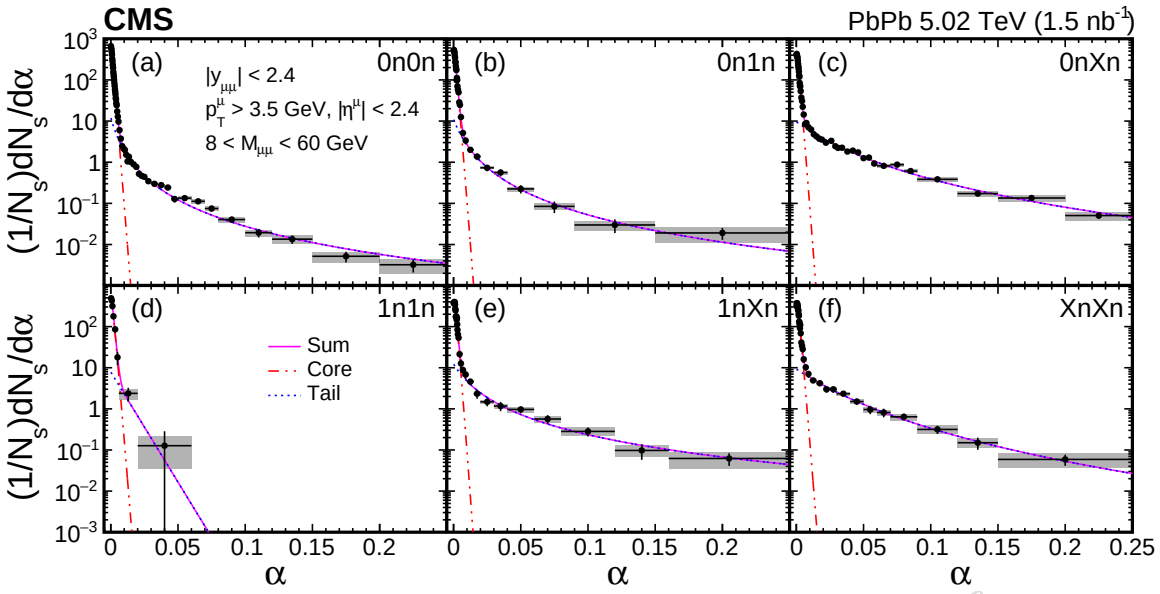

Figure 1: Neutron multiplicity dependence of α spectra from $\gamma\gamma \to \mu^+\mu^-$ within the CMS acceptance for $8 < M_{\mu\mu} < 60$ GeV in PbPb collisions at $\sqrt{s_{\mathrm{NN}}} = 5.02$ TeV. The α distributions are normalized to unit integral over their measured range. The dot-dot dashed line depicts the core contribution while the dotted line represents the tail contribution. The vertical lines on data points depict the statistical uncertainties, while the systematic uncertainties are shown as gray boxes.

produce more neutrons in the forward region. A rapidity dependence of the α distribution is also investigated and documented in the supplemental material. In the 0nXn class, the tail contribution in the same rapidity hemisphere with Xn is larger than that in the opposite rapidity hemisphere. A similar trend has been observed in Ref. [21].

To investigate a possible impact parameter dependence of the initial photon p_{T}, the core contribution to the α distribution is decoupled from the tail contribution using a two-component empirical fit function,

$$\begin{aligned} \text{core} &: c_1 \times e^{-\alpha/c_2 + c_3 \times \alpha^{0.25}} \\ \text{tail} &: t_1 \times (1 + (t_2/t_3) \times \alpha)^{-t_3}, \end{aligned} \tag{2}$$

except for the case of 1n1n, where a simple exponential function is used for the tail component ~~due to~~ given the limited number of events. A binned χ^2 minimization is performed using the function's integral in each bin to account for the finite histogram binning effect. The average acoplanarity ($\langle\alpha^{\mathrm{core}}\rangle$) of $\mu^+\mu^-$ pairs from the core component is then calculated from the fit function.

The measured α distribution and $\langle\alpha^{\mathrm{core}}\rangle$ of $\mu^+\mu^-$ pairs are affected by several sources of systematic uncertainty arising from contamination of hadronic collisions, the dissociative pileup correction, neutron multiplicity classification, and the fit procedure. The uncertainty of hadronic contamination is estimated by removing the requirement of selected events only containing two muon candidates and is found to be <1.1%. To estimate the systematic uncertainty associated with the HF noise threshold, the leading HF energy deposit is tightened to 5 GeV for both UPC and zero bias triggered events. The difference from the nominal result is quoted as the systematic uncertainty and contributes <2.7%. The uncertainty arising from impure 1n class selection

(<0.7%) is estimated by subtracting the contributions of 2n events selected with tight energy cuts according to the 2n contamination probability. The systematic uncertainty associated with contamination of photoproduced Υ (~0.6%) is estimated by comparing α distributions from STARlight between pure $\gamma\gamma \to \mu^+\mu^-$ and $\gamma\gamma \to \mu^+\mu^-$ mixed with photoproduced coherent $\Upsilon(1S)$ according to the relative yield ratio of $\Upsilon(1S)$ over $\gamma\gamma \to \mu^+\mu^-$ as estimated from data. The systematic uncertainty ~~on~~ in $\langle\alpha^{\text{core}}\rangle$ associated with the binned χ^2 fit procedure is estimated by varying the bin width of α distributions and is found to be less than 4.0%. The total systematic uncertainties are derived from a quadrature sum of the aforementioned systematic sources and found to be ~1.3–5.1% on $\langle\alpha^{\text{core}}\rangle$. For the $\langle M_{\mu\mu}\rangle$ results, a second order polynomial function is fit to the mass spectrum, excluding the mass region $9 < M_{\mu\mu} < 11\,\text{GeV}$, to interpolate the contribution of $\gamma\gamma$ scattering in the Υ mass region. The systematic uncertainty related to this procedure is estimated by comparing the nominal result to one obtained by a third-order polynomial function fit. Together with the aforementioned systematic sources, the total systematic uncertainty ~~to~~ in $\langle M_{\mu\mu}\rangle$ is below 1.8% across all neutron multiplicity classes.

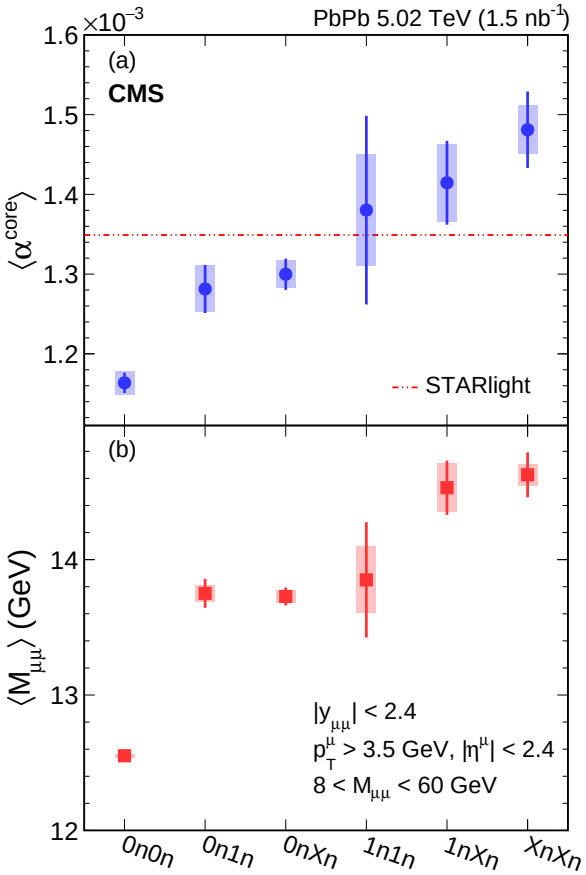

Figure 2: Neutron multiplicity dependence of $\langle\alpha^{\text{core}}\rangle$ (a) and $\langle M_{\mu\mu}\rangle$ of $\mu^+\mu^-$ pairs (b) within the CMS acceptance in the mass region $8 < M_{\mu\mu} < 60\,\text{GeV}$. The vertical lines on data points depict the statistical uncertainties, while the systematic uncertainties of the data are shown as shaded areas.

The neutron multiplicity dependence of $\langle\alpha^{\text{core}}\rangle$ of $\mu^+\mu^-$ pairs in ultra-peripheral PbPb collisions at $\sqrt{s_{\text{NN}}} = 5.02\,\text{TeV}$ within the CMS acceptance is shown in Fig. 2 (a), ~~within the CMS acceptance~~ in the mass region $8 < M_{\mu\mu} < 60\,\text{GeV}$. ~~Strong~~ A strong neutron multiplicity dependence of $\langle\alpha^{\text{core}}\rangle$ is clearly observed, while the $\langle\alpha^{\text{core}}\rangle$ predicted by STARlight is constant 1.348×10^{-3} as indicated by the dashed-dotted line in Fig. 2 (a). Meanwhile, the neu-

tron ~~multiplicity integrated~~ multiplicity-integrated $\langle \alpha^{\text{core}} \rangle$ is measured to be (1227 $\pm$ 7 (stat.) $\pm$ 8 (syst.))$\times 10^{-6}$, which is 9.0% lower than the STARlight prediction. In general, the $\langle \alpha^{\text{core}} \rangle$ in data becomes larger as the emitted neutron multiplicity increases. The $\langle \alpha^{\text{core}} \rangle$ in $X\text{n}X\text{n}$ events (small $\langle b \rangle$) is about 5.3 standard deviations (σ) larger than that in 0n0n events (large $\langle b \rangle$). A constant fit to $\langle \alpha^{\text{core}} \rangle$ yields a χ^2 with a p-value corresponding to 5.7σ. This observation demonstrates that initial photons producing $\mu^+\mu^-$ pairs have a significant impact parameter dependence of their p_{T}, which impacts the p_{T} and acoplanarity of muon pairs in the final state. This initial-state contribution must be properly taken into account when exploring possible final-state EM effects from a hot QGP medium formed in hadronic ~~heavy-ion~~ heavy ion collisions [24, 25].

In Fig. 2 (b), the average invariant mass ($\langle M_{\mu\mu} \rangle$) of all muon pairs from $\gamma\gamma$ scattering in ultra-peripheral PbPb collisions at $\sqrt{s_{\text{NN}}}$ = 5.02 TeV within the CMS acceptance is also studied as a function of the neutron multiplicity, ~~within the CMS acceptance~~ in the mass region $8 < M_{\mu\mu} < 60$ GeV. Again, strong neutron multiplicity dependence of $\langle M_{\mu\mu} \rangle$ is observed and the $\langle M_{\mu\mu} \rangle$ in $X\text{n}X\text{n}$ events is larger than that in 0n0n events with a significance clearly exceeding 5σ. Meanwhile, the data disfavor the hypothesis of no neutron multiplicity dependence of $\langle M_{\mu\mu} \rangle$ with a significance much greater than 5σ. As the muon pair invariant mass is largely determined by the initial photon energy, this observation suggests that the average energy of photons involved in photon-induced interactions tends to be larger in collisions with smaller impact parameters, a conclusion similar to that previously drawn for the initial photon p_{T}.

In summary, first measurements of $\gamma\gamma \to \mu^+\mu^-$ production as a function of forward neutron multiplicity in ultra-peripheral lead-lead collisions at a nucleon-nucleon center-of-mass energy of 5.02 TeV are reported. Strong neutron multiplicity dependence of azimuthal correlations between muon pairs produced from $\gamma\gamma$ scattering is observed. A significant broadening of back-to-back azimuthal correlations from the leading-order $\gamma\gamma \to \mu^+\mu^-$ process is seen as the neutron multiplicity in the forward region increases. A similar trend of increasing average invariant mass of muon pairs with neutron multiplicity is also observed. These measurements demonstrate that initial photon energy and transverse momentum in photon-induced interactions of heavy ion collisions have impact parameter dependence. These results call for new theoretical efforts to improve the modeling of photon-induced interactions and make fundamental impacts in many aspects. For instance, future searches for ~~quark-gluon-plasma induced~~ quark-gluon-plasma-induced electromagnetic interactions should carefully consider these initial broadening effects when forming a baseline model to compare against many aspects of high-energy nuclear physics.

Acknowledgments

We congratulate our colleagues in the CERN accelerator departments for the excellent performance of the LHC and thank the technical and administrative staffs at CERN and at other CMS institutes for their contributions to the success of the CMS effort. In addition, we gratefully acknowledge the computing centres and personnel of the Worldwide LHC Computing Grid for delivering so effectively the computing infrastructure essential to our analyses. Finally, we acknowledge the enduring support for the construction and operation of the LHC and the CMS detector provided by the following funding agencies: BMBWF and FWF (Austria); FNRS and FWO (Belgium); CNPq, CAPES, FAPERJ, FAPERGS, and FAPESP (Brazil); MES (Bulgaria); CERN; CAS, MoST, and NSFC (China); COLCIENCIAS (Colombia); MSES and CSF (Croatia); RPF (Cyprus); SENESCYT (Ecuador); MoER, ERC IUT, PUT and ERDF (Estonia); Academy of Finland, MEC, and HIP (Finland); CEA and CNRS/IN2P3 (France); BMBF, DFG, and HGF

(Germany); GSRT (Greece); NKFIA (Hungary); DAE and DST (India); IPM (Iran); SFI (Ireland); INFN (Italy); MSIP and NRF (Republic of Korea); MES (Latvia); LAS (Lithuania); MOE and UM (Malaysia); BUAP, CINVESTAV, CONACYT, LNS, SEP, and UASLP-FAI (Mexico); MOS (Montenegro); MBIE (New Zealand); PAEC (Pakistan); MSHE and NSC (Poland); FCT (Portugal); JINR (Dubna); MON, RosAtom, RAS, RFBR, and NRC KI (Russia); MESTD (Serbia); SEIDI, CPAN, PCTI, and FEDER (Spain); MOSTR (Sri Lanka); Swiss Funding Agencies (Switzerland); MST (Taipei); ThEPCenter, IPST, STAR, and NSTDA (Thailand); TUBITAK and TAEK (Turkey); NASU (Ukraine); STFC (United Kingdom); DOE and NSF (USA).

References

[1] E. J. Williams, "Nature of the high energy particles of penetrating radiation and status of ionization and radiation formulae", *Phys. Rev.* **45** (1934) 729, doi:10.1103/PhysRev.45.729.

[2] STAR Collaboration, "Probing Extreme Electromagnetic Fields with the Breit-Wheeler Process", arXiv:1910.12400.

[3] C. A. Bertulani and G. Baur, "Electromagnetic Processes in Relativistic Heavy Ion Collisions", *Phys. Rept.* **163** (1988) 299, doi:10.1016/0370-1573(88)90142-1.

[4] G. Baur et al., "Coherent $\gamma\gamma$ and γA interactions in very peripheral collisions at relativistic ion colliders", *Phys. Rept.* **364** (2002) 359, doi:10.1016/S0370-1573(01)00101-6, arXiv:hep-ph/0112211.

[5] G. Baur, K. Hencken, and D. Trautmann, "Electron-Positron Pair Production in Relativistic Heavy Ion Collisions", *Phys. Rept.* **453** (2007) 1, doi:10.1016/j.physrep.2007.09.002, arXiv:0706.0654.

[6] C. A. Bertulani, S. R. Klein, and J. Nystrand, "Physics of ultra-peripheral nuclear collisions", *Ann. Rev. Nucl. Part. Sci.* **55** (2005) 271, doi:10.1146/annurev.nucl.55.090704.151526, arXiv:nucl-ex/0502005.

[7] A. J. Baltz, "The Physics of Ultraperipheral Collisions at the LHC", *Phys. Rept.* **458** (2008) 1, doi:10.1016/j.physrep.2007.12.001, arXiv:0706.3356.

[8] S. Klein and P. Steinberg, "Photonuclear and Two-photon Interactions at High-Energy Nuclear Colliders", arXiv:2005.01872.

[9] ATLAS Collaboration, "Evidence for light-by-light scattering in heavy-ion collisions with the ATLAS detector at the LHC", *Nature Phys.* **13** (2017) 852, doi:10.1038/nphys4208, arXiv:1702.01625.

[10] ATLAS Collaboration, "Observation of light-by-light scattering in ultraperipheral Pb+Pb collisions with the ATLAS detector", *Phys. Rev. Lett.* **123** (2019) 052001, doi:10.1103/PhysRevLett.123.052001, arXiv:1904.03536.

[11] CMS Collaboration, "Evidence for light-by-light scattering and searches for axion-like particles in ultraperipheral PbPb collisions at $\sqrt{s_{\mathrm{NN}}} = 5.02$ TeV", *Phys. Lett. B* **797** (2019) 134826, doi:10.1016/j.physletb.2019.134826, arXiv:1810.04602.

[12] B. L. Berman and S. C. Fultz, "Measurements of the giant dipole resonance with monoenergetic photons", *Rev. Mod. Phys.* **47** (1975) 713, doi:10.1103/RevModPhys.47.713.

[13] M. Broz, J. G. Contreras, and J. D. Tapia Takaki, "A generator of forward neutrons for ultra-peripheral collisions: $\mathbf{n}^{\mathrm{O}}_{\mathrm{O}}\mathbf{n}$", arXiv:1908.08263.

[14] STAR Collaboration, "Coherent ρ^0 production in ultraperipheral heavy ion collisions", *Phys. Rev. Lett.* **89** (2002) 272302, doi:10.1103/PhysRevLett.89.272302, arXiv:nucl-ex/0206004.

[15] STAR Collaboration, "Production of e^+e^- pairs accompanied by nuclear dissociation in ultra-peripheral heavy ion collision", *Phys. Rev. C* **70** (2004) 031902, doi:10.1103/PhysRevC.70.031902, arXiv:nucl-ex/0404012.

[16] STAR Collaboration, "Coherent diffractive photoproduction of ρ^0 mesons on gold nuclei at 200 GeV/nucleon-pair at the Relativistic Heavy Ion Collider", *Phys. Rev. C* **96** (2017) 054904, doi:10.1103/PhysRevC.96.054904, arXiv:1702.07705.

[17] PHENIX Collaboration, "Photoproduction of J/ψ and of high mass e^+e^- in ultra-peripheral Au+Au collisions at $\sqrt{s_{_{NN}}}$ = 200 GeV", *Phys. Lett. B* **679** (2009) 321, doi:10.1016/j.physletb.2009.07.061, arXiv:0903.2041.

[18] ALICE Collaboration, "Coherent J/ψ photoproduction in ultra-peripheral Pb-Pb collisions at $\sqrt{s_{NN}} = 2.76$ TeV", *Phys. Lett. B* **718** (2013) 1273, doi:10.1016/j.physletb.2012.11.059, arXiv:1209.3715.

[19] ALICE Collaboration, "Charmonium and e^+e^- pair photoproduction at mid-rapidity in ultra-peripheral Pb-Pb collisions at $\sqrt{s_{\mathrm{NN}}}$=2.76 TeV", *Eur. Phys. J. C* **73** (2013) 2617, doi:10.1140/epjc/s10052-013-2617-1, arXiv:1305.1467.

[20] ALICE Collaboration, "Coherent J/ψ photoproduction at forward rapidity in ultra-peripheral Pb-Pb collisions at $\sqrt{s_{\mathrm{NN}}} = 5.02$ TeV", *Phys. Lett. B* **798** (2019) 134926, doi:10.1016/j.physletb.2019.134926, arXiv:1904.06272.

[21] CMS Collaboration, "Coherent J/ψ photoproduction in ultra-peripheral PbPb collisions at $\sqrt{s_{\mathrm{NN}}} = 2.76$ TeV with the CMS experiment", *Phys. Lett. B* **772** (2017) 489, doi:10.1016/j.physletb.2017.07.001, arXiv:1605.06966.

[22] CMS Collaboration, "Measurement of exclusive Y photoproduction from protons in pPb collisions at $\sqrt{s_{\mathrm{NN}}} = 5.02$ TeV", *Eur. Phys. J. C* **79** (2019) 277, doi:10.1140/epjc/s10052-019-6774-8, arXiv:1809.11080.

[23] CMS Collaboration, "Measurement of exclusive $\rho(770)^0$ photoproduction in ultraperipheral pPb collisions at $\sqrt{s_{\mathrm{NN}}} = 5.02$ TeV", *Eur. Phys. J. C* **79** (2019) 702, doi:10.1140/epjc/s10052-019-7202-9, arXiv:1902.01339.

[24] STAR Collaboration, "Low-p_T e^+e^- pair production in Au+Au collisions at $\sqrt{s_{NN}}$ = 200 GeV and U+U collisions at $\sqrt{s_{NN}}$ = 193 GeV at STAR", *Phys. Rev. Lett.* **121** (2018) 132301, doi:10.1103/PhysRevLett.121.132301, arXiv:1806.02295.

[25] ATLAS Collaboration, "Observation of centrality-dependent acoplanarity for muon pairs produced via two-photon scattering in Pb+Pb collisions at $\sqrt{s_{\mathrm{NN}}} = 5.02$ TeV with the ATLAS detector", *Phys. Rev. Lett.* **121** (2018) 212301, doi:10.1103/PhysRevLett.121.212301, arXiv:1806.08708.

[26] ALICE Collaboration, "Measurement of an excess in the yield of J/ψ at very low p_{T} in Pb-Pb collisions at $\sqrt{s_{\mathrm{NN}}}$ = 2.76 TeV", *Phys. Rev. Lett.* **116** (2016) 222301, doi:10.1103/PhysRevLett.116.222301, arXiv:1509.08802.

[27] STAR Collaboration, "Observation of excess J/ψ yield at very low transverse momenta in Au+Au collisions at $\sqrt{s_{\rm NN}} = 200$ GeV and U+U collisions at $\sqrt{s_{\rm NN}} = 193$ GeV", *Phys. Rev. Lett.* **123** (2019) 132302, doi:10.1103/PhysRevLett.123.132302, arXiv:1904.11658.

[28] S. Klein, A. H. Mueller, B.-W. Xiao, and F. Yuan, "Acoplanarity of a Lepton Pair to Probe the Electromagnetic Property of Quark Matter", *Phys. Rev. Lett.* **122** (2019) 132301, doi:10.1103/PhysRevLett.122.132301, arXiv:1811.05519.

[29] W. Zha, J. D. Brandenburg, Z. Tang, and Z. Xu, "Initial transverse-momentum broadening of Breit-Wheeler process in relativistic heavy-ion collisions", *Phys. Lett. B* **800** (2020) 135089, doi:10.1016/j.physletb.2019.135089, arXiv:1812.02820.

[30] S. Klein, A. H. Mueller, B.-W. Xiao, and F. Yuan, "Lepton Pair Production Through Two Photon Process in Heavy Ion Collisions", arXiv:2003.02947.

[31] CMS Collaboration, "Performance of CMS Muon Reconstruction in pp Collision Events at $\sqrt{s} = 7$ TeV", *JINST* **7** (2012) P10002, doi:10.1088/1748-0221/7/10/P10002, arXiv:1206.4071.

[32] CMS Collaboration, "The CMS Experiment at the CERN LHC", *JINST* **3** (2008) S08004, doi:10.1088/1748-0221/3/08/S08004.

[33] CMS Collaboration, "Observation and studies of jet quenching in PbPb collisions at nucleon-nucleon center-of-mass energy = 2.76 TeV", *Phys. Rev. C* **84** (2011) 024906, doi:10.1103/PhysRevC.84.024906, arXiv:1102.1957.

[34] S. R. Klein et al., "STARlight: A Monte Carlo simulation program for ultra-peripheral collisions of relativistic ions", *Comput. Phys. Commun.* **212** (2017) 258, doi:10.1016/j.cpc.2016.10.016, arXiv:1607.03838.

[35] GEANT4 Collaboration, "GEANT4: A Simulation toolkit", *Nucl. Instrum. Meth. A* **506** (2003) 250, doi:10.1016/S0168-9002(03)01368-8.

[36] I. A. Pshenichnov et al., "Mutual heavy ion dissociation in peripheral collisions at ultrarelativistic energies", *Phys. Rev. C* **64** (2001) 024903, doi:10.1103/PhysRevC.64.024903, arXiv:nucl-th/0101035.

[37] I. A. Pshenichnov, "Electromagnetic excitation and fragmentation of ultrarelativistic nuclei", *Phys. Part. Nucl.* **42** (2011) 215, doi:10.1134/S1063779611020067.

[38] ALICE Collaboration, "Measurement of the Cross Section for Electromagnetic Dissociation with Neutron Emission in Pb-Pb Collisions at $\sqrt{s_{NN}}$ = 2.76 TeV", *Phys. Rev. Lett.* **109** (2012) 252302, doi:10.1103/PhysRevLett.109.252302, arXiv:1203.2436.